

Reversing non-local transport through a superconductor by electromagnetic excitations

A. Levy Yeyati, F.S. Bergeret and A. Martín-Rodero
*Departamento de Física Teórica de la Materia Condensada C-V,
 Universidad Autónoma de Madrid, E-28049 Madrid, Spain*

T.M. Klapwijk

Kavli Institute of Nanoscience, Delft University of Technology, Lorentzweg 1, 2628 CJ Delft, The Netherlands

Superconductors connected to normal metallic electrodes at the nanoscale provide a potential source of non-locally entangled electron pairs. Such states would arise from Cooper pairs splitting into two electrons with opposite spins tunnelling into different leads. In an actual system the detection of these processes is hindered by the elastic transmission of individual electrons between the leads, yielding an opposite contribution to the non-local conductance. Here we show that electromagnetic excitations on the superconductor can play an important role in altering the balance between these two processes, leading to a dominance of one upon the other depending on the spatial symmetry of these excitations. These findings allow to understand some intriguing recent experimental results and open the possibility to control non-local transport through a superconductor by an appropriate design of the experimental geometry.

In 1964 A.F. Andreev proposed a mechanism to explain the conversion of quasiparticle currents into supercurrents at the interface between a normal metal (N) and a superconductor (S) [1]. In the so-called Andreev reflection mechanism an incident electron from the N region is reflected as a hole and a Cooper pair is created on the superconductor. This process can be viewed as the transfer of two electrons with opposite spins from N to S where they combine to form a Cooper pair. In multiterminal N/S structures a non-local version of this process where the electrons are injected from two spatially separated electrodes, can take place [2, 3, 4]. The possibility to detect these *crossed Andreev reflection* (CAR) processes have attracted a lot of interest since it provides a natural mechanism to produce non-locally entangled electron pairs in a condensed matter device [5, 6, 7, 8, 9]. Unfortunately, a competing mechanism known as elastic cotunnelling (EC) in which electrons are transmitted elastically between the two electrodes, is always present in actual devices yielding an opposite contribution to the non-local conductance. The theory, in fact, predicts that for BCS superconductors weakly coupled to non-magnetic leads the contributions of EC and CAR processes to the non-local conductance tend to cancel each other [10, 11]. Spin polarisation due to magnetism in the leads could break this cancellation [10, 12], an idea that has been explored in recent experiments [13]. Surprisingly, a different set of experiments by Russo et al. [14] has shown that even for the case of non-magnetic leads coupled to the superconductor by tunnel junctions the subgap non-local conductance can be appreciably large, exhibiting an intriguing behaviour in which either process can dominate depending on the applied voltage range.

In this work we analyse the influence of electron interactions in the transport properties of this type of multiterminal N/S structures. A key feature of this analysis is played by low energy collective excitations which appear in superconductors of reduced dimensionality [15]. When an electron tunnels into the superconductor it can excite such low energy modes which alters the balance between EC and CAR processes. Moreover, depending on the spatial symmetry of these excitations either CAR or EC processes can be suppressed, leading to a change in the sign of the non-local conductance as a function of the applied voltage. These findings provide an explanation to the experimental results of Ref. [14] and suggest new strategies for the detection of CAR induced transport in nanostructures.

A generic set-up for measuring the non-local resistance is shown in Fig.1a. It represents a superconducting region attached to three normal electrodes. Two of the leads (labelled 1 and 2 in Fig.1a) are used to inject a current while the voltage drop is measured on the third one. As illustrated in Fig.1c, EC processes produce and injection of electrons into the third lead while CAR processes withdraw them from it, which yields opposite contributions to the non-local resistance [16]. On the other hand both processes decay on the superconducting coherence length ξ , which can range between 10 and 100 nm for typical superconductors used in experiments [13, 14].

The importance of interactions in breaking the balance between EC and CAR processes can be understood by considering the case where the S region is sufficiently small and can be characterised by a finite charging energy E_c . As it is sketched in Fig.1c, EC processes take place through a virtual state which will be shifted upwards by the Coulomb energy. The process, however, would not be blocked for any value of the applied voltage as the initial and final states have the same energy. In contrast, CAR processes demand that two electrons tunnel into the S region forming a Cooper pair, a process which requires an extra energy of $4E_c$. Thus, the non-local conductance has a finite (negative) value for a voltage V smaller than $4E_c/e$ where EC processes dominate, while it vanishes for $eV > 4E_c$.

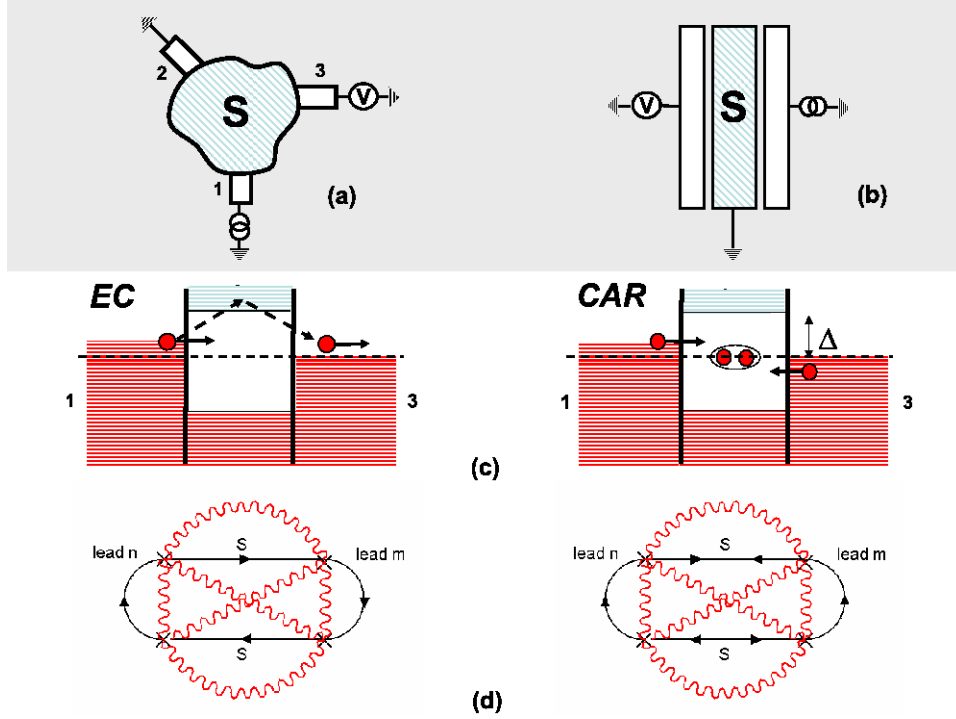


FIG. 1: Top panel: a) Schematic representation of a generic multiterminal geometry where a superconducting region is coupled to several metallic leads and b) Double planar N/S/N junction geometry studied in Ref. [14]. Middle panel (c): Pictorial description of EC and CAR processes in energy space. Lower panel (d): Feynman diagrams corresponding to the calculation of the non-local conductance to fourth order taking into account interactions mediated by the electromagnetic environment. Full lines with an arrow represent the normal and anomalous propagators and wavy lines indicate phase correlators.

when both processes cancel each other.

For a quantitative analysis of the influence of interactions we describe the system by a Hamiltonian $\hat{H} = \hat{H}_S + \hat{H}_{leads} + \hat{H}_T + \hat{H}_{env}$. The first three terms correspond to the electronic degrees of freedom. \hat{H}_S is the usual BCS Hamiltonian for the S region and \hat{H}_{leads} describes the normal leads which we label with an index n . The tunnelling of electrons between the leads and the superconductor is described by $\hat{H}_T = \sum_n \hat{H}_{T,n}$, with

$$\hat{H}_{T,n} = \sum_{\sigma} \int_{S_n} d^2r \left[v_n \hat{\psi}_{ln,\sigma}^{\dagger}(\vec{r}) \hat{\psi}_{sn,\sigma}(\vec{r}) e^{i\hat{\phi}_n(\vec{r})} + \text{h.c.} \right], \quad (1)$$

where the integral is taken over the junction area S_n , $\hat{\psi}_{ln,\sigma}^{\dagger}(\vec{r})$ and $\hat{\psi}_{sn,\sigma}^{\dagger}(\vec{r})$ are electron creation operators on the two sides of junction and $\hat{\phi}_n(\vec{r})$ is the corresponding phase drop which is conjugate to the charge density on the junction $\hat{Q}_n(\vec{r})$, i.e. $[\hat{\phi}_n(\vec{r}), \hat{Q}_n(\vec{r}')] = ie\delta(\vec{r} - \vec{r}')$. The dynamics of these phase operators is determined by the Hamiltonian \hat{H}_{env} describing the electromagnetic environment characterising the actual experimental set-up. It is important to note that, due to the typical distances between the leads in the experiments, which are not much larger than ξ , correlations between voltage fluctuations on different junctions cannot be neglected, i.e. correlation functions of the type $\langle \hat{\phi}_n \hat{\phi}_m \rangle$, with $n \neq m$ are non-zero. In addition, the reduced dimensions of the S region can give rise to the presence of collective modes within the superconducting gap, which can dominate the behaviour of the phase correlations.

To obtain the transport properties of this model we use a combination of Keldysh and Nambu formalisms which is well adapted to analyse non-equilibrium situations in the presence of superconductivity [17]. The contributions from EC and CAR processes to the non-local conductance G_{nm} , i.e. the variation of the current through lead n due to a voltage applied on lead m , in the tunnel limit is represented by the type of diagrams shown in Fig.1d. The solid lines with an arrow represent the electron propagators, while the wavy lines describe the coupling with the environment, i.e. they denote the phase correlators of the type $\langle e^{i\hat{\phi}_n} e^{-i\hat{\phi}_m} \rangle$. Let us first consider the simplest case where the environment can be characterised by a single electromagnetic mode of frequency ω_0 . One can further assume that the leads are coupled to the S region through point contacts as illustrated in Fig.2. Two opposite situations can be

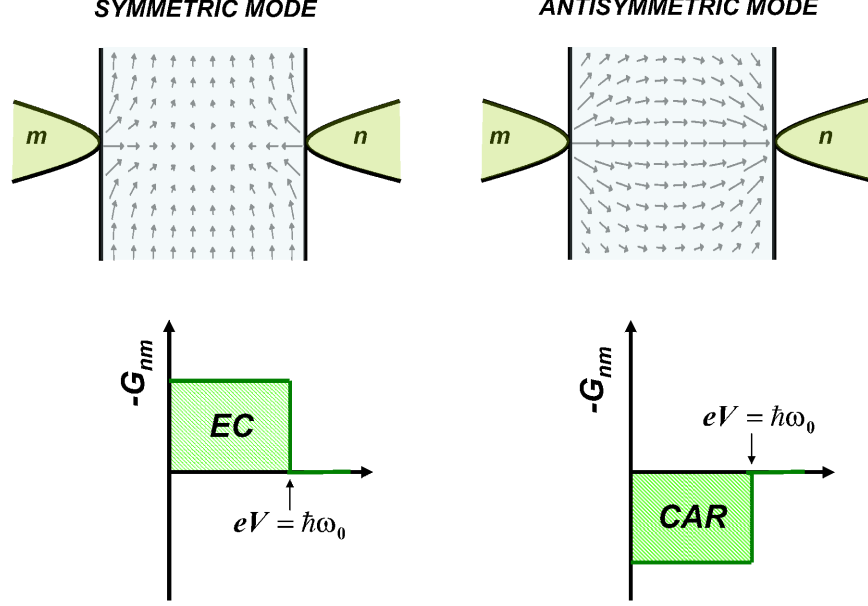


FIG. 2: Pictorial representation of the effect of interactions mediated by electromagnetic modes of different symmetry on the non-local conductance between two point contacts. The arrows represent the phase gradient within the superconductor. While symmetric modes tend to suppress CAR processes the antisymmetric ones suppress the EC contribution.

distinguished depending on the spatial symmetry of the electromagnetic mode under consideration: it can lead to either symmetric or antisymmetric voltage fluctuations on the two junctions. In the symmetric case, assuming that $\hbar\omega_0$ is much smaller than the superconducting gap Δ , and for S in the clean limit, at zero temperature we obtain (see Supplementary Information)

$$G_{nm} = -\frac{G_n G_m}{G_0} \frac{e^{-2R/\xi}}{(k_F R)^2} e^{-2z_0} \sum_{n_1 \dots n_6} \left[\prod_{i=1}^6 \frac{(z_0)^{n_i}}{n_i!} \right] \theta(eV - \sum_{i=1}^4 n_i \hbar\omega_0) [(-1)^{n_3+n_4} \cos^2(k_F R) - (-1)^{n_5+n_6} \sin^2(k_F R)]. \quad (2)$$

Here $G_{n(m)}$ is the normal conductance of the junction n (m), R the distance separating the leads, k_F is the Fermi wavevector, $G_0 = 2e^2/h$ is the conductance quantum and V is the voltage applied on lead m . The term proportional to $\cos^2(k_F R)$ corresponds to the EC contribution while the $\sin^2(k_F R)$ term arises from CAR processes. The parameter $z_0 = E_c/\hbar\omega_0$, where $E_c = e^2/2C$ is the charging energy on the tunnel junctions, measures the coupling to the electromagnetic mode. The indexes n_i , with i ranging from 1 to 6 denote the number of quanta associated to the phase correlators on each diagram in Fig.1d, 5 and 6 corresponding to the more external wavy lines. The behaviour predicted by Eq. (2) becomes more clear in the $z_0 \ll 1$ limit where it can be simplified to obtain

$$G_{nm} \simeq -\frac{G_n G_m}{G_0} \frac{e^{-2R/\xi}}{(k_F R)^2} [\cos^2(k_F R) - (1 - z_0 \theta(\hbar\omega_0 - eV)) \sin^2(k_F R)]. \quad (3)$$

It is worth noticing that this expression reproduces the non-interacting result [10] for $z_0 = 0$, where a complete cancellation between CAR and EC contributions takes place upon averaging over the Fermi wavelength scale. For finite but small z_0 the balance between EC and CAR is broken: for eV smaller than $\hbar\omega_0$ the CAR processes become suppressed and non-local transport is dominated by the EC contribution, while for $eV > \hbar\omega_0$ both contributions tend to cancel, as in the non-interacting case. The suppression of the CAR contribution is due to the impossibility of such processes to occur without producing a real excitation of the environment, as in the constant charging energy example.

The situation is the opposite in the case of an antisymmetric mode. The analog of expression to Eq. (2) for this case is obtained by an exchange of the indexes n_3, n_4 with n_5, n_6 in the last factor within brackets. As a consequence EC

(instead of CAR) processes will be suppressed at low voltages. The different effect of symmetric and antisymmetric modes is schematically illustrated in Fig.2.

We now consider the case of a planar geometry similar to the one in the experiments of Ref. [14] (Fig.1b), consisting of a superconducting layer of thickness $d \gtrsim \xi$ coupled to two normal leads by tunnel junctions. The cross section of the junctions in Ref. [14] was relatively large ($\sim 30 \mu m^2$), which allows to describe them as infinite planes [18]. The electromagnetic environment in this situation is characterised by the presence of propagating modes along the S/N junctions, which can be derived from the following model Hamiltonian

$$\hat{H}_{env} = \left(\frac{\hbar}{2e}\right)^2 \int d^3r \frac{(\nabla \hat{\phi})^2}{2Ld} + \int d^2r \frac{1}{2C_{\square}} \left(\hat{Q}_L^2 + \hat{Q}_R^2\right), \quad (4)$$

where the term containing the phase gradient describes the kinetic energy associated to the supercurrents in the S film, L being its total inductance, while the second term is the Coulomb energy of the charge accumulated on the junctions (assumed to be symmetric with capacitance C_{\square} per unit area and with cross section \mathcal{S}). In writing this Hamiltonian we are assuming that long range Coulomb interactions are screened by the normal electrodes acting as ground planes [19]. The low energy modes which result from this model correspond to symmetric and antisymmetric voltage fluctuations on the junctions, with dispersion relations $\omega_1(\vec{q}) = c_s \sqrt{(q \tanh qd)/d}$ and $\omega_2(\vec{q}) = c_s \sqrt{q/(d \tanh qd)}$, where \vec{q} is the wavevector in the direction parallel to the film and $c_s = 1/\sqrt{LC_{\square}}$. Notice that for small q the symmetric mode exhibits a linear dispersion with phase velocity c_s while the antisymmetric one tends to a finite frequency $\omega_0 = c_s/d$ in the limit $q \rightarrow 0$. This description of the low energy modes captures the essential features of a detailed calculation based on Maxwell equations for the double planar junction geometry (see Supplementary information).

One can roughly estimate the order of magnitude of the parameters in \hat{H}_{env} for the experimental situation. Thus, C_{\square} can be obtained from the typical charging energy for an oxide barrier tunnel junction $E_c \mathcal{S} \sim 1 \mu eV \times \mu m^2$ and L can be estimated as $\mu_0 \lambda^2/d$, λ being the field penetration depth [20]. The actual value of λ for a Nb film is strongly dependent on its thickness, degree of disorder and it is also influenced by the properties of the non-superconducting substrate on which it is deposited [21]. Reported values range between 100 nm and 1 μm for $d \sim 10 - 100$ nm [21, 22]. Within this range of parameters the lowest energy of the antisymmetric mode $\hbar\omega_0$ can be of the order of a few meV, i.e. comparable to the superconducting gap in Nb, even for the smaller film thickness analysed in Ref. [14].

To obtain the non-local conductance G_{LR} measured at the left interface when a voltage V is applied on the right junction we extend the theory developed for the single mode case, linearising with respect to the coupling parameters $z_{1,2}(\vec{q}) = E_c/\hbar\omega_{1,2}(\vec{q})$, which is justified for the range of parameters estimated above. We thus obtain

$$G_{LR} = 4\pi \frac{G_L G_R}{\mathcal{S} k_F^2 G_0} \text{Ei}(-2d/\xi) \sum_{\vec{q}, \alpha=1,2} (-1)^{\alpha} z_{\alpha}(\vec{q}) [(N(\omega_{\alpha}(\vec{q}) + 1) (F(\omega_{\alpha}(\vec{q})) + 1) + N(\omega_{\alpha}(q)) (F(-\omega_{\alpha}(q)) + 1)], \quad (5)$$

where $G_{L,R}$ is the normal conductance of each junction, $F(\epsilon) = \int d\omega \frac{\partial f(\omega)}{\partial \omega} [f(\omega + \epsilon - V) + f(\omega + \epsilon + V)]$ is a thermal smearing kernel arising from the Fermi distribution $f(\omega)$ while $N(\omega_{\alpha})$ is the Bose distribution function. The planar geometry leads to the factor $\text{Ei}(-2d/\xi)$, where Ei denotes the exponential integral function. This leads to an exponential decay of the non-local conductance when increasing d .

In order to understand the behaviour of G_{LR} as a function of voltage it is convenient to first analyse the contribution arising from a given wavevector q . This is illustrated in the upper panel of Fig.3 for $T = 10^{-2}\Delta$ and $\hbar\omega_0 = 0.4\Delta$. The behaviour for the different wavevectors is qualitatively similar: for $eV < \hbar\omega_1, \hbar\omega_2$ the EC processes dominate, while CAR become more important in the voltage window $\hbar\omega_1 < eV < \hbar\omega_2$ and finally both contributions cancel for $eV > \hbar\omega_2$.

The sum of all contributions yields a non-local conductance which is dominated by EC processes at $V \rightarrow 0$ and decreases almost linearly with V until $eV \simeq \hbar\omega_0$. At this point the onset of antisymmetric modes produces a strong suppression of EC processes and there is a change of sign in G_{LR} (CAR dominates). We can therefore associate $\hbar\omega_0$ with the crossing energy from EC to CAR dominated regimes. The lower panel of Fig.3 shows the voltage dependence of G_{LR} for different temperatures. As can be observed, the imbalance between EC and CAR processes driven by the electromagnetic modes is less pronounced for increasing temperature. The characteristic temperature for the suppression of the non-local conductance is set by $\hbar\omega_0/k_B$. This behaviour is in qualitative agreement with the results of Ref.[14]. Moreover, the magnitude of the non-local conductance predicted by our model is in reasonable agreement with the experimental values. For instance, the ratio $G_{LR}/G_{L,R}^s$ between the non-local and the direct conductances in the superconducting state at zero voltage and zero temperature is $0.75 \text{Ei}(-2d/\xi)(E_c \mathcal{S} \omega_0 / \hbar c_s^2)$ which yields values $\sim 10^{-3}$ close to the experimental ones for the parameters estimated above. A more quantitative description of the experimental results will be presented elsewhere.

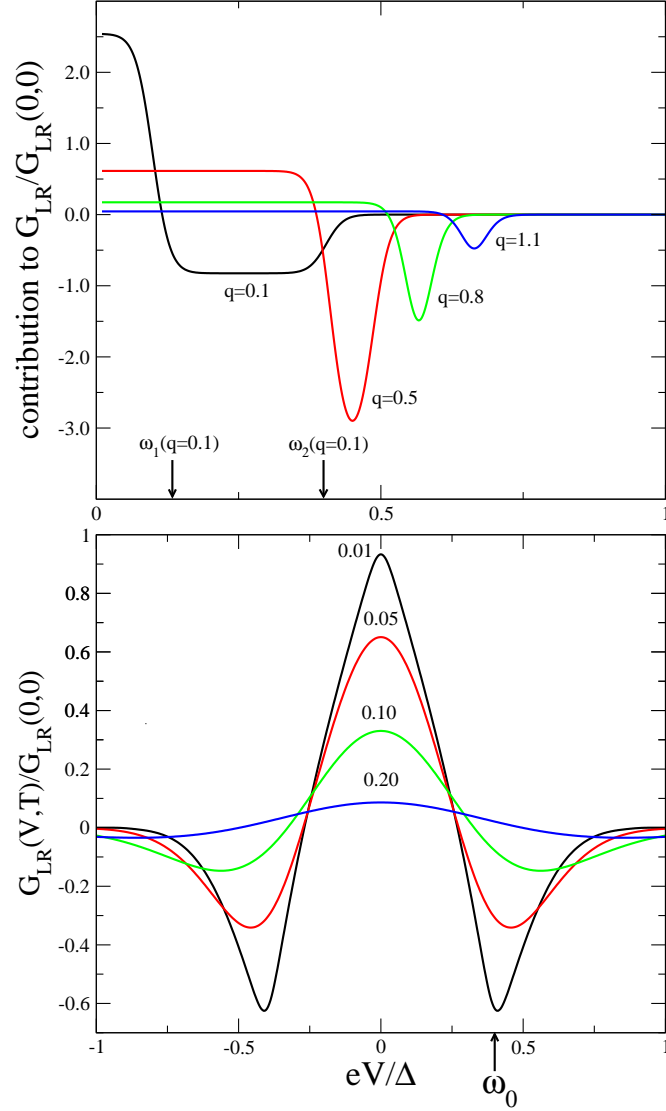


FIG. 3: Upper panel: Contribution to the non-local conductance from modes with a given wavevector in the double planar junction geometry for $k_B T = 0.01\Delta$ and $\hbar\omega_0 = 0.4\Delta$. The values of q are given in units of $\Delta/\hbar c_s$. The arrows indicate the energy of symmetric and antisymmetric modes for $q = 0.1$. Lower panel: Temperature and voltage dependence of the total non-local conductance. The temperature values are given in units of Δ/k_B . The arrow indicates the energy $\hbar\omega_0$ for the lowest antisymmetric mode.

In conclusion we have shown that electron interactions mediated by electromagnetic excitations lead to an imbalance between EC and CAR processes. Electromagnetic modes can either suppress CAR or EC processes depending on their spatial symmetry. Taking into account that these low energy excitations are strongly dependent on the geometrical characteristics of the multiterminal device, these findings open the possibility to control non-local transport processes through a superconductor by an appropriate design of the experimental set-up. For instance, one possibility would be to introduce an additional tunnel junction inside the superconducting film in the experimental geometry of Ref. [14]. This N/S/S/N nanostructure would allow to control the dispersion relation of the electromagnetic modes by varying the Josephson coupling between the S layers by means of a magnetic field. Let us finally point out that the high sensitivity of non-local transport to the electromagnetic modes could be used as a tool to analyse these excitations in hybrid nanostructures.

The authors would like to thank fruitful discussions and correspondence with D. Beckmann, A. Morpurgo, S. Russo, C. Urbina, D. Esteve, W. Herrera, R.C. Monreal and J.C. Cuevas.

-
- [1] Andreev, A. F. The thermal conductivity of the intermediate state in superconductors. *Sov. Phys. JETP* **19**, 1228 (1964).
 - [2] Byers, J. M., & Flatté, M. E. Probing Spatial Correlations with Nanoscale Two-Contact Tunneling. *Phys. Rev. Lett.* **74**, 306-309 (1995).
 - [3] Hartog S. G. den et. al., Transport in MultiTerminal Normal-Superconductor Devices: Reciprocity Relations, Negative and Nonlocal Resistances, and Reentrance of the Proximity Effect. *Phys. Rev. Lett.* **77**, 4954 (1996).
 - [4] Deutscher, G. & Feinberg, D. Coupling superconducting-ferromagnetic point contacts by Andreev reflections. *Appl. Phys. Lett.* **76**, 487-489 (2000).
 - [5] Recher, P., Sukhorukov, E. V. & Loss, D. Andreev tunneling, Coulomb blockade, and resonant transport of nonlocal spin-entangled electrons. *Phys. Rev. B* **63**, 165314 (2001).
 - [6] Chtchelkatchev, N. M., Blatter, G., Lesovik, G.B. & Martin, T. Bell inequalities and entanglement in solid-state devices. *Phys. Rev. B* **66**, 161320 (2002).
 - [7] Bena, C., Vishveshwara, S., Balents, L. & Fisher, M. P. A. Quantum Entanglement in Carbon Nanotubes. *Phys. Rev. Lett.* **89**, 037901 (2002).
 - [8] Samuelsson, P., Sukhorukov, E. V. & Büttiker, M. Orbital Entanglement and Violation of Bell Inequalities in Mesoscopic Conductors. *Phys. Rev. Lett.* **91**, 157002 (2003).
 - [9] Prada, E. & Sols, F. Entangled electron current through finite size normal-superconductor tunneling structures. *Eur. Phys. J. B* **40**, 379 (2004).
 - [10] Falci, G., Feinberg, D. & Hekking, F. W. J. Correlated tunneling into a superconductor in a multiprobe hybrid structure. *Europhys. Lett.* **54**, 255 (2001).
 - [11] Feinberg, D. Andreev scattering and cotunneling between two superconductor-normal metal interfaces: the dirty limit. *Eur. Phys. J. B* **36**, 419-422 (2003).
 - [12] Mélin, R. & Feinberg, D. Sign of the crossed conductances at a ferromagnet/superconductor/ferromagnet double interface. *Phys. Rev. B* **70**, 174509-174518 (2004).
 - [13] Beckmann, D., Weber, H. B. & Löhneysen, H. v. Evidence for Crossed Andreev Reflection in Superconductor-Ferromagnet Hybrid Structures. *Phys. Rev. Lett.* **93**, 197003 (2004).
 - [14] Russo, S., Kroug, M., Klapwijk, T. M. & Morpurgo, A. F. Experimental Observation of Bias-Dependent Nonlocal Andreev Reflection. *Phys. Rev. Lett.* **95**, 027002 (2005).
 - [15] Low energy collective excitations in thin superconducting filaments were first analysed by Mooij, J. E. & Schön, G. Propagating plasma mode in thin superconducting filaments. *Phys. Rev. Lett.* **55**, 114 (1985).
 - [16] Conventionally the CAR contribution to the non-local conductance is taken as positive, which corresponds to a negative contribution to the non-local resistance. See Ref. [10].
 - [17] See for instance Levy Yeyati, A. Cuevas, J. C. & Martín-Rodero, A. Dynamical Coulomb Blockade of Multiple Andreev Reflections. *Phys. Rev. Lett.* **95**, 056804 (2005) and references therein.
 - [18] The possibility to observe interaction effects in large area tunnel junctions between normal metals was demonstrated by Pierre, F. et. al. Electrodynamic Dip in the Local Density of States of a Metallic Wire. *Phys. Rev. Lett.* **86**, 1590 (2001). These results were explained in terms of standard dynamical Coulomb blockade theory. This theory in its usual form is unable to account for the effects of interactions on non-local transport through superconductors discussed in the present work.
 - [19] Hermele, M., Rafael, G., Fisher, M.P.A. & Goldbart, P. M. Fate of the Josephson effect in thin-film superconductors. *Nature Physics* **1**, 117 (2005).
 - [20] Orlando T.P., Delin K.E., *Foundations of Applied Superconductivity*, Reading, M.A., Addison-Wesley (1991).
 - [21] Gubin A.I. et. al., Dependence of magnetic penetration depth on the thickness of superconducting Nb thin films, *Phys. Rev. B* **72**, 064503 (2005).
 - [22] Parage F., M.M. Doria and O. Buisson, Plasma modes in periodic two-dimensional superconducting-wire networks, *Phys. Rev. B* **58**, R8921 (1998).